Full Paper

New Phytologist

Spread of self-compatibility constrained by an intrapopulation crossing barrier

Amanda K. Broz[1], Armeda Simpson-Van Dam[1], Alejandro Tovar-Méndez[2], Matthew W. Hahn[3,4], Bruce McClure[5] and Patricia A. Bedinger[1]

[1]Department of Biology, Colorado State University, Fort Collins, CO 80523-1878, USA; [2]Elemental Enzymes, 1685 Galt Ind. Blvd, St Louis, MO 63132, USA; [3]Department of Biology, Indiana University, Bloomington, IN 47405, USA; [4]Department of Computer Science, Indiana University, Bloomington, IN 47405, USA; [5]Department of Biochemistry, University of Missouri-Columbia, Columbia, MO 65211, USA

Author for correspondence:
Amanda K. Broz
Email: amandabroz@gmail.com

Received: *16 January 2021*
Accepted: *9 April 2021*

New Phytologist (2021) **231:** 878–891
doi: 10.1111/nph.17400

Key words: intrapopulation reproductive barrier, mating system transition, pollen–pistil interactions, self-compatibility, self-incompatibility, *Solanum habrochaites*, wild tomato species.

Summary

- Mating system transitions from self-incompatibility (SI) to self-compatibility (SC) are common in plants. In the absence of high levels of inbreeding depression, SC alleles are predicted to spread due to transmission advantage and reproductive assurance.
- We characterized mating system and pistil-expressed SI factors in 20 populations of the wild tomato species *Solanum habrochaites* from the southern half of the species range.
- We found that a single SI to SC transition is fixed in populations south of the Rio Chillon valley in central Peru. In these populations, SC correlated with the presence of the *hab-6* S-haplotype *that encodes a low activity S-RNase protein. We identified a single population segregating for SI/SC and hab-6*. Intrapopulation crosses showed that *hab-6* typically acts in the expected codominant fashion to confer SC. However, we found one specific S-haplotype (*hab-10*) that consistently rejects pollen of the *hab-6* haplotype, and results in SI *hab-6*/*hab-10* heterozygotes.
- We suggest that the *hab-10* haplotype could act as a genetic mechanism to stabilize mixed mating in this population by presenting a disadvantage for the *hab-6* haplotype. This barrier may represent a mechanism allowing for the persistence of SI when an SC haplotype appears in or invades a population.

Introduction

The transition from outcrossing to self-fertilization is one of the most common evolutionary changes in flowering plants (Darwin, 1876; Stebbins, 1974; Igic *et al.*, 2008). Outcrossing can be favored by selection (Goldberg *et al.*, 2010) and is retained throughout plant lineages. In many plant species, outcrossing is enforced by genetic systems of self-incompatibility (SI) (de Nettancourt, 1977; Takayama & Isogai, 2005; Fujii *et al.*, 2016). Phylogenetic studies suggest that a small number of SI systems arose very early in the history of angiosperms (Steinbachs & Holsinger, 2002; Allen & Hiscock, 2008; Ramanauskas & Igić, 2017). Thus, in outcrossing plant families, SI is presumed to be the ancestral state and the transition from SI to self-compatibility (SC) due to mutational loss of SI factors is generally thought to be irreversible (Goldberg & Igić, 2012; Igic & Busch, 2013).

In the absence of other selective forces, a selfing allele is predicted to spread to fixation within a population due simply to the 3 : 2 transmission advantage over an outcrossing allele (Fisher, 1941). Modeling suggests that factors such as inbreeding depression or pollen and seed discounting (loss of outcross siring and seed production in selfing individuals) must be extremely high to counteract the spread of selfing via SC (Charlesworth & Charlesworth, 1979; Porcher & Lande, 2005; Busch & Delph, 2012). In addition, SC individuals have a fitness advantage over SI individuals when mates or pollinators are limiting, resulting in selection for SC (Baker, 1955; Busch & Schoen, 2008; Pannell *et al.*, 2015). In an extreme example, a single SC individual could establish a new population, whereas at least two cross-compatible SI individuals would be required.

The degree of outcrossing versus selfing is critical to population genetic structure and can influence the ability of a population to adapt to a changing environment (Charlesworth & Wright, 2001; Barrett *et al.*, 2014). Because SI enforces outcrossing, it maintains heterozygosity within a population and presumably contributes to long-term genetic resiliency and persistence. However, in populations with selfing individuals, deleterious recessive alleles that result in inbreeding depression are more likely to be exposed and purged over time (Lande & Schemske, 1985). Thus, the advantages of reproduction via self-pollination are balanced against the potential costs of reduced genetic diversity and inbreeding depression, which may lead to more rapid extinction in SC vs SI lineages (Lande & Schemske, 1985; Charlesworth, 2003; Busch & Delph, 2012; Igic & Busch, 2013;

Wright *et al.*, 2013). In natural populations, numerous selective pressures influence mating system dynamics, which can promote or limit the spread of SC, often resulting in the maintenance of mixed SI/SC populations (Goodwillie *et al.*, 2005).

A number of evolutionary and ecological studies of mating system transitions have focused on species within the Solanaceae (Igic *et al.*, 2006; Goldberg *et al.*, 2010; Stone *et al.*, 2014; Vallejo-Marín *et al.*, 2014; Broz *et al.*, 2017b). In this plant family, SI is gametophytic, wherein the haploid genotype of the pollen (male gametophyte) determines compatibility with the diploid genotype of the female as the pollen tube grows through the style towards the ovaries. This type of SI is the most common system of incompatibility in flowering plants (Silva & Goring, 2001) and is controlled largely by genes that are physically clustered in a region known as the *S*-locus (McClure *et al.*, 2011; Fujii *et al.*, 2016; Bedinger *et al.*, 2017). At the *S*-locus, male- and female-expressed genes are tightly linked and inherited together; thus, the *S*-identity of a diploid individual is most appropriately regarded as a combination of two *S*-haplotypes.

The female *S*-determinant in this system is a hypervariable cytotoxic S-RNase (McClure *et al.*, 1989) that is highly expressed and secreted in pistils, and is taken up by pollen tubes as they grow through the transmitting tract within the pistil. The male *S*-determinant consists of multiple *S*-locus F-box genes (SLFs) that are highly expressed in pollen (Sijacic *et al.*, 2004). Current models suggest that multiple SLFs act cooperatively to recognize and detoxify all S-RNases excepting the one encoded at their own *S*-locus (Kubo *et al.*, 2010). Therefore, at least in the Solanaceae, an *S*-haplotype is comprised of allelic variants encoding a single S-RNase and numerous (*c.* 16–23) SLFs (Williams *et al.*, 2014; Kubo *et al.*, 2015; Li & Chetelat, 2015; Wu *et al.*, 2020). Moreover, the Solanaceae S-RNase-based SI system also requires additional factors that do not contribute to *S*-specificity and are not encoded at the *S*-locus. These include female-side factors such as the small asparagine-rich HT proteins, the 120 kDa glycoprotein and others (McClure *et al.*, 1999; Hancock *et al.*, 2005; Goldraij *et al.*, 2006; Jiménez-Durán *et al.*, 2013). Pollen-side non-*S*-locus factors include components of the E3 ubiquitin ligase complex that interact with SLFs; the *S*-phase kinase associated protein-like 1 (SKP1) and Cullin 1 (CUL1) (Zhao *et al.*, 2010; Li & Chetelat, 2014).

The collaborative non-self-recognition model explains the specificity of S-RNase-based SI in Solanaceae, wherein a pistil barrier is circumvented by a suite of pollen resistance factors (Kubo *et al.*, 2010; Bedinger *et al.*, 2017). In this model, non-self S-RNases are taken up by growing pollen tubes and are recognized and detoxified by one or more SLFs. However, self-S-RNases are not recognized, which results in pollen RNA degradation and ultimately pollen tube rejection. As a result of these interactions, *S*-specific pollen rejection occurs between individuals that contain the same *S*-haplotype. Multiple *S*-haplotypes are maintained within populations and species by negative frequency-dependent selection, as rare haplotypes have a mating advantage.

The tomato clade (*Solanum* Section Lycopersicon) is well suited for studies of mating system transitions, since the switch from SI to SC has occurred multiple times (Igic *et al.*, 2008; Broz *et al.*, 2017b). These transitions often occur at species margins, consistent with selection for reproductive assurance, as predicted by Baker's Law (Baker, 1955; Baker, 1967). In the wild tomato species *Solanum habrochaites*, SI to SC transitions have occurred at both the northern and southern species margins (Martin, 1963; Rick *et al.*, 1979; Rick & Chetelat, 1991; Covey *et al.*, 2010; Markova *et al.*, 2016; Broz *et al.*, 2017b). At least two transitions have occurred at the northern species margin, with different *S-RNase* alleles having low or no expression of S-RNase (Broz *et al.*, 2017b; Miller, 2018). In the southernmost population of *S. habrochaites*, an S-RNase (hab-6) is expressed in styles, but it exhibits very low levels of activity compared to S-RNases found in SI populations (Covey *et al.*, 2010). The *hab-6* allele is thus hypothesized to result in SC, as S-RNase activity is required for RNA degradation, resulting in rejection of self-pollen tubes.

We investigated the SI → SC transition in southern *S. habrochaites* populations and traced the distribution of the *hab-6* S-RNase *allele. Our results are consistent with a single mating system transition associated with hab-6* that is fixed in southern populations. We identified a single population segregating for SI/SC and for *hab-6*. In this population we characterized an *S*-haplotype encoding an active S-RNase that was co-dominant with *hab-6*, producing SC plants, as expected in gametophytic S-RNase-based SI. Surprisingly, we also identified a different *S*-haplotype in this population encoding an active S-RNase (*hab-10*) that, when paired with any other haplotype tested, rejects pollen of the *hab-6* haplotype. We propose that the presence of the *hab-10* *S*-haplotype *limits the spread of the SC haplotype, allowing SI and SC haplotypes to coexist within this population.*

Materials and Methods

Solanum habrochaites plant material and growth

The range of *Solanum habrochaites* (S. Knapp & D. M. Spooner) extends from central Ecuador to south-central Peru, where it often occupies river valleys in the Andean highlands (Peralta *et al.*, 2008). The *S. habrochaites* accessions (hereafter referred to as populations) used in this study cover the southern part of the range, from near Cajamarca, Peru to near Nazca, Peru (Table 1; Fig. 1). Seeds from all populations were acquired from the C. M. Rick Tomato Genetic Resource Center (TGRC) at University of California, Davis (www.tgrc.ucdavis.edu).

Seeds were sterilized according to recommendations from TGRC, planted into 4-inch (101.6 mm) pots containing ProMix-BX, and grown under glasshouse conditions (16 h : 8 h, light : dark photoperiod, at 26°C and 18°C, respectively) until they were 6–12 inches (150 to 300 mm) tall. For mating system experiments plants were transplanted to outdoor agricultural fields at Colorado State University in late May. When seed set was required, plants were transferred to 1-gallon (4.55 l) pots and maintained under glasshouse conditions or placed in growth chambers (10 h : 14 h, light : dark photoperiod) to induce flowering.

Table 1 *Solanum habrochaites* accessions used in this study.

Population	Collection site	Province/department	Latitude (°N)	Longitude (°W)	Elevation (m asl)
LA1353	Contumaza	Cajamarca	−7.367	−78.800	2650
LA1777	Rio Casma	Ancash	−9.550	−77.667	3216
LA1978	Colca	Ancash	−10.108	−77.484	2450
LA1557	Huaral to Cerro de Pasco	Lima	−11.220	−76.630	3173
LA1772	Rio Chillon	Lima	−11.483	−76.650	2500
LA0094	Yangas to Canta	Lima	−11.517	−76.683	1600–2100
LA1648	Above Yaso	Lima	−11.551	−76.715	1800
LA0361	Canta	Lima	−11.567	−76.730	1600
LA1298	East of Yaso, Rio Chillon	Lima	−11.583	−76.750	1600
LA1560	Matucana	Lima	−11.850	−76.383	2400
LA1295	Surco	Lima	−11.883	−76.442	2100
LA1753	Surco	Lima	−11.885	−76.440	2300
LA1691	Yauyos	Lima	−12.460	−75.918	2900
LA2722	Puente Auco	Lima	−12.589	−75.958	1890
LA1681	Mushka	Lima	−12.750	−75.833	2450
LA1731	Rio San Juan	Huancavelica	−13.202	−75.575	2000
LA1721	Ticrapo Viejo	Huancavelica	−13.435	−75.465	2100
LA1918	Llauta	Ayacucho	−14.250	−74.917	2600
LA1928	Ocana	Ayacucho	−14.399	−74.823	2660
LA1927	Ocobamba	Ayacucho	−14.450	−74.817	2540

All accessions were originally collected in Peru and seeds were acquired from the C. M. Rick Tomato Genetic Resource Center (TGRC, University of California, Davis, www.tgrc.ucdavis.edu). m asl, meters above sea level.

Mating system assessment and controlled pollinations

Mating system was assessed and verified for at least three plants from each population. Initially plants were screened for self-fruit production in agricultural fields by self-pollinating flowers on at least two inflorescences per plant and monitoring self-fruit set. Inflorescences were covered with nylon mesh bags to prevent pollen deposition from other sources. Because field plants flowered in late summer, self-fruits often did not reach maturity before frost; thus, the presence of highly swollen ovaries (> 0.5 cm in diameter) was regarded as successful fruit set. When an individual did not set self-fruit, self-pollen tube growth through styles was utilized to assess mating system as described in Broz *et al.* (2017b). Briefly, self-pollinations were performed, and styles were collected 48 h after pollination, stained with Aniline Blue Fluorochrome and imaged at ×5 magnification. Pollinations were considered compatible if three or more pollen tubes reached the base of the style.

Polymerase chain reaction (PCR) amplification and sequence comparison of *hab-6 S-RNase* allele and homologs

We hypothesized that the *hab-6* allele, which had previously been identified in a single southern population (LA1927) (Covey *et al.*, 2010) was responsible for SC at the southern species range margin. We screened a minimum of three individuals per population for the presence of the *hab-6 S-RNase* allele using gene specific primers (1927F/1927R). Genomic DNA was extracted from leaf tissue using the Qiagen DNeasy Plant Mini-Kit. All primers are listed in Supporting Information Table S1.

We amplified and sequenced the 5′ UTR and full-length coding region of *hab-6* from populations originating within each of the major river valleys in the southern *S. habrochaites* range, as well as an individual of *Solanum chilense* known to harbor the *S2 S-RNase* allele (*S. chilense* seed generously provided by Boris Igic). The 5′UTR primer (AB5F) was based on the genomic sequence of the *Solanum peruvianum SP11 S-RNase* (GenBank U28795), which is 98.4% identical to *hab-6*. Polymerase chain reaction was performed using Econotaq Plus Green Mastermix (Lucigen, Madison, WI, USA). Genomic DNA and deduced amino acid sequences were aligned using MUSCLE (http://www.ebi.ac.uk/Tools/msa/muscle/ (Madeira *et al.*, 2019)), signal peptide analysis was performed using TARGETP (http://www.cbs.dtu.dk/services/TargetP/ (Almagro Armenteros *et al.*, 2019)), and protein structures were modeled using SWISS-MODEL (https://swissmodel.expasy.org/ (Waterhouse *et al.*, 2018)).

Genotyping individuals for analysis of *hab-6* at the *S*-locus

We assessed whether *hab-6* segregated as would be predicted for a gene at the *S*-locus by genotyping progeny of specific crosses in which *S-RNase* alleles of the females are well-characterized. Females in the crosses were either *Solanum lycopersicum* (cultivars VF36 or Pearson), which contain the loss-of-function 'Lyco' *S-RNase* allele with a 94 bp insert (Li & Chetelat, 2015), or *S. habrochaites* SC accession LA0407, which contains the nonexpressed *LhgSRN-1 S-RNase* allele (Covey *et al.*, 2010). Buds of glasshouse grown plants were emasculated the day before opening and pollinated after 24 h using pollen from an individual that was heterozygous for the *hab-6* and *hab-10 S-RNase* alleles. Seeds from these crosses were planted and genomic DNA was extracted from young seedlings in 200 mM Tris-HCl pH 9.0, 250 mM NaCl, 25 mM EDTA, and 1% SDS, followed by precipitation in isopropanol. Polymerase chain reaction to detect known *S-RNase* alleles in progeny was performed as described in the previous

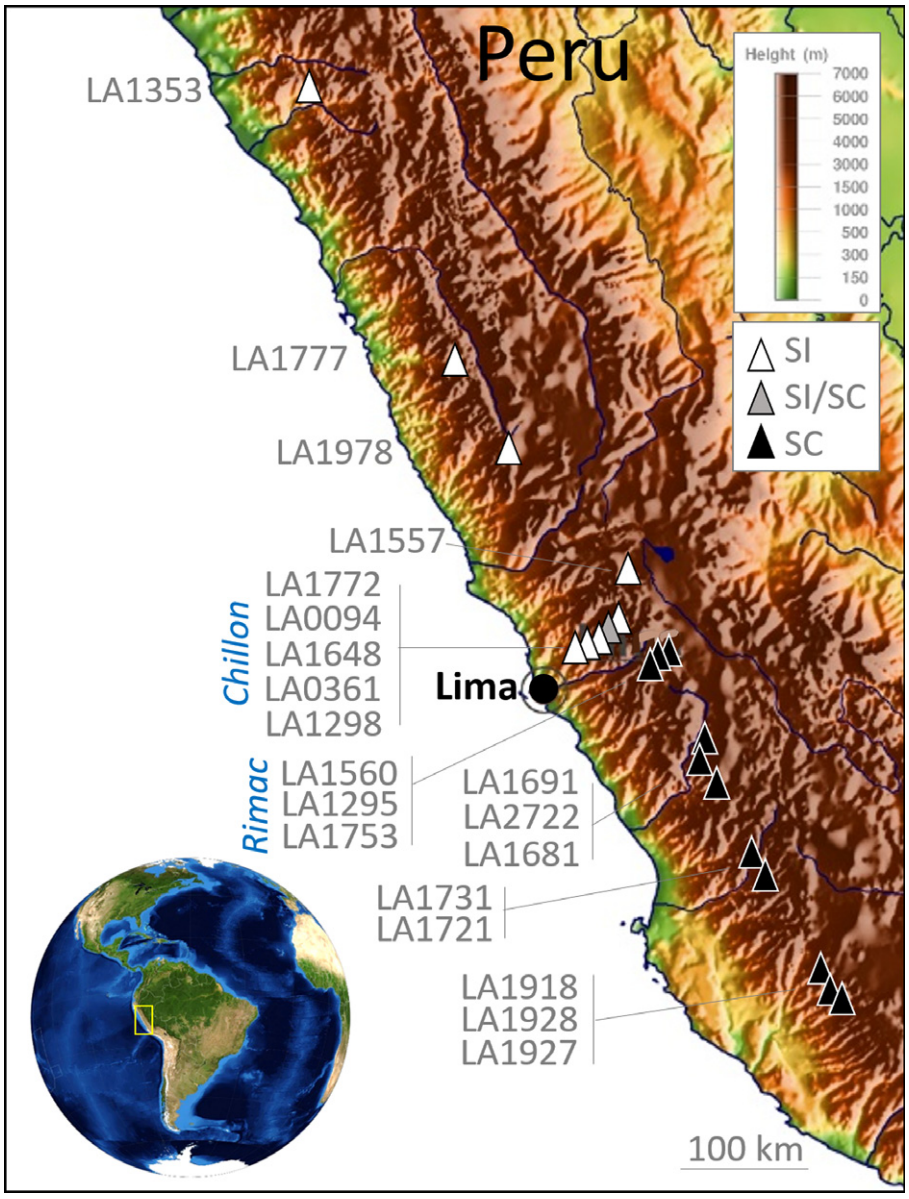

Fig. 1 Mating system distribution in southern *Solanum habrochaites* populations. Mating system was assessed in this study by fruit set and pollen tube growth through styles after self-pollination for 17 populations of *S. habrochaites*; designations for three populations (LA1772, LA1298 and LA1731) are those of the Tomato Genetic Resource Center (TGRC). River valley names are designated in blue. SC, self-compatible; SI, self-incompatible; SI/SC, mixed population.

section. Genotyping results were analyzed using the Freeman–Halton extension of Fisher's exact test ($n = 128$; no plants contained both alleles, 51 *hab-6* only, 77 *hab-10* only): if *hab-6* is at the *S*-locus expected (0, 64, 64) vs observed (0, 77, 51), $P = 0.13$; if *hab-6* is unlinked to the *S*-locus expected (32, 48, 48) vs observed (0, 77, 51), $P = 4 \times 10^{-11}$.

Transcriptome sequencing and analysis of stylar RNA

We performed transcriptome analysis on individuals from one population at the center of the SC distribution (LA2722) to determine if the *hab-6* haplotype was fixed. Unpollinated styles from three individuals were separately collected into RNAlater (Qiagen), and total RNA was extracted and pooled in an equimolar ratio as described in Broz *et al.* (2017a). RNA quality control, library preparation and bioinformatics were performed by the Indiana University Center for Genomics and Bioinformatics. Sequencing of the unfragmented whole transcriptome libraries was performed on an Illumina MiSeq (San Diego, CA, USA) to generate 250 bp paired end reads. The raw transcriptome data are available on the NCBI SRA database (BioProject PRJNA310635). Data processing, analysis and identification of *S-RNase* sequences are described in Methods S1.

Detection of stylar S-RNase and HT-proteins

Expression of S-RNases, the specific hab-6 S-RNase and HT-proteins was assessed by immunostaining protein gel blots of stylar extracts from at least three individuals from most populations (as described in Broz *et al.*, 2017b). For each individual tested, protein equivalent to 0.2 mg (S-RNase) or 1.5 mg (HT-protein) fresh weight was separated by electrophoresis, blotted, and immunostained as previously described (Covey *et al.*, 2010). Antibodies for the S-RNase conserved C-2 domain, tSRNC2

(Chalivendra *et al.*, 2013) and HT-protein (Broz *et al.*, 2017b) have been described previously. An antibody specific for hab-6 S-RNase was prepared to the peptide VPRSSHTVDKIKKTIRSV-amide (21st Century Biochemicals, Marlborough, MA, USA), and used at a dilution of 1 : 5000 for immunoblotting.

Deglycosylation of hab-6 S-RNase

To determine whether the hab-6 S-RNase is glycosylated, which could influence activity, deglycosylation followed by sodium dodecyl-sulfate polyacrylamide gel electrophoresis (SDS-PAGE) analyses were performed. Briefly, hab-6 S-RNase was partially purified by adsorption of extracts (extraction buffer, 0.05 M Tris, 1% 2-mercaptoethanol, pH 7) from 15 mg of pistils from LA1927 to S-Sepharose (25 µl). After washing five times, proteins were eluted with the same buffer plus 0.2 M NaCl. Eluted proteins were treated with 8 U peptide-N-glycanase F for 1, 10 or 90 min according to the manufacturer's instructions (cat. no. P0704S; New England Biolabs) before immunoblotting analysis.

Identification of additional *S-RNase* alleles in a population segregating for *hab-6*

We identified a single *S. habrochaites* population (LA0094) that was segregating for SI/SC and *hab-6*, and screened individuals from this population for additional *S-RNase* alleles. Styles were harvested from open flowers, RNA was extracted using the RNeasy Plant Mini-kit (Qiagen) and reverse transcription was performed using the iScript cDNA synthesis kit (Bio-Rad). Degenerate PCR primers were used to amplify *S-RNase* alleles *hab-9* and *hab-10* from cDNA of individual plants (as in Covey *et al.*, 2010). Polymerase chain reaction products were separated in a 1% agarose gel, purified using the Qia-Quick Gel Extraction Kit (Qiagen) and cloned into the pJET vector (Thermo Scientific, Waltham, MA, USA). At least three clones were selected for sequencing. An additional *S-RNase* allele (*hab-11*) was amplified using primers previously designed to a putative/pseudogene *S-RNase* sequence (*hab-8*) (Miller, 2018), and the PCR amplicon was sequenced. To understand the genetic interaction between *S*-haplotypes found in population LA0094, we performed intrapopulation crosses. Buds were emasculated the day before opening and pollinated after 24 h. Pistils were either harvested after 48 h to examine pollen tube growth through styles or left on the plant until fruits/seeds had matured. All pollinations were conducted in a growth chamber.

Results

A single self-incompatibility to self-compatibility mating system transition occurred in *Solanum habrochaites* in central Peru

All individuals from all *S. habrochaites* populations collected within and south of the Rio Rimac river valley (near the Surco district in Peru; latitude 76.383°S) were capable of SC fruit set. Mating system assessment of southern *S. habrochaites* populations (Fig. 1; Table 2) was mostly congruent with TGRC reports. However, our analyses found that all individuals tested from accessions LA1560, LA1295, LA1753 (all located in the Rio Rimac valley) and LA2722 set fruit after self-pollinations, inconsistent with their previous designation as SI. Interestingly, an older collection from the Rio Rimac valley (LA0120, Surco) was reported as SC (Martin, 1963). We found both SI and SC individuals in population LA0094 from the Rio Chillon valley, which was previously designated SC by TGRC, but reported as SI by Martin (1963). In all populations capable of setting self-fruit, fruit set from self-pollinations was low (< 50% of attempts were successful), consistent with previous studies of southern populations (Martin, 1963; Rick *et al.*, 1979).

Controlled self-crosses were performed for populations that did not set self-fruit (i.e. presumably SI), and self-pollen tube growth through styles was examined. Overall, self-pollen tubes were actively rejected in individuals from these populations. However, a limited number of pollen tubes (3–10) were occasionally observed in the ovaries of individuals from two populations (LA1353 and LA0316). In these cases, pollen tube rejection varied both between individuals within a population and between different flowers from the same individual. Although these individuals were classified as variable (noted in Table 2), the populations were still considered SI (Fig. 1) because no fruits were formed.

The low-activity hab-6 S-RNase correlates with a self-compatibility mating system

We screened a minimum of three individuals per population from 20 populations for the *hab-6* allele, which had previously been identified in population LA1927 (Covey *et al.*, 2010). We found that *hab-6* was present in every individual of the 11 southern-most populations tested, including LA1927, all of which were SC. We also identified SC individuals in segregating population LA0094 that contained the *hab-6* allele (Fig. 2; Tables 2, S2). We chose one SC population (LA2722) from the center of the SC range to generate a stylar transcriptomic library and found that *hab-6* was expressed at a high level in styles (FPKM values *c.* 11 000) as is typical for S-RNases. Further, it was the only *S-RNase* expressed in a pool of three individuals, suggesting that the allele is homozygous in this population.

Immunostaining of protein gel blots of stylar extracts using a general S-RNase antibody (tSRNC2) confirmed that all individuals tested, whether SI or SC, expressed S-RNase proteins (representative samples shown in Fig. 3). Further, an antibody designed to specifically identify hab-6 revealed a characteristic double banding pattern in individuals from SC populations that contained the *hab-6* allele (Table 2; Fig. 3). Two individuals of SI population LA1777 also expressed proteins that were recognized by the hab-6 antibody (Table 2; Fig. 3), but transcriptome analyses showed that these individuals expressed an S-RNase only 83.6% identical to hab-6 (Fig. S1). In summary, the presence and expression of the *hab-6* allele was strictly correlated with SC in southern *S. habrochaites* populations.

Table 2 Presence of *hab-6* S-RNase allele and hab-6 protein in *Solanum habrochaites* populations based on polymerase chain reaction (PCR) and immunoblotting.

Accession (N to S)	Mating system	Positive PCR amplification of *hab-6* allele	Positive Western blot with hab-6 antibody
LA1353	SI[a]	0/8	0/3
LA1777	SI	0/11	2/10[d]
LA1978	SI	0/15	NT
LA1557	SI	0/7	0/3
LA1772	SI[b]	0/6	NT
LA0094	SI/SC	16/22	6/12
LA1648	SI	0/10	0/3
LA0361	SI[a]	0/15	NT
LA1298	SI[b]	0/3	NT
LA1560	SC	6/6	NT
LA1295	SC[c]	11/11	3/3
LA1753	SC	11/11	7/7
LA1691	SC	7/7	10/10
LA2722	SC	14/14	11/11
LA1681	SC	3/3	3/3
LA1731	SC[b]	3/3	NT
LA1721	SC	9/9	5/5
LA1918	SC	6/6	3/3
LA1928	SC	9/9	4/4
LA1927	SC	10/10	3/3

Mating system was determined using a combination of self-fruit set and pollen-tube growth assays. Allele-specific primers were used to test for amplification of the *hab-6* allele from genomic DNA, and stylar extract protein blots were probed with the hab-6 S-RNase antibody (no. of individuals testing positive / total no. of individuals tested). NT, not tested; SC, self-compatible; SI, self-incompatible.

[a]Individuals within the population showed variability in pollen tube growth.

[b]Mating system was not assessed in this study and Tomato Genetic Resource Center (TGRC) designation is shown.

[c]Only images of pollen tube growth were obtained for SC mating system designation.

[d]Banding pattern of reactive protein differed from southern SC accessions.

In silico and biochemical analyses of hab-6 S-RNase

The entire *hab-6* sequence from 5′ of the start codon to the stop codon was amplified and sequenced from selected individuals in populations collected from each river valley throughout the southern distribution (Fig. S2) All gDNA sequences contained the single intron characteristic of Solanaceous *S-RNases* (Ramanauskas & Igić, 2017). Comparison of *hab-6* sequences between accessions revealed a single nonsynonymous SNP in the two southern-most populations analyzed (LA1721 and LA1927) that would lead to an L/F polymorphism in the signal peptide region (Figs 4, S2).

We compared the hab-6 deduced amino acid sequence with two closely related functional alleles. The deduced amino acid sequence of hab-6 contains the S-RNase conserved domains C1–C5 (including the two catalytic histidine residues), and is over 97% identical to S-RNases: S11 from SI *S. peruvianum* (Miller & Kostyun, 2011) and S2 from SI *S. chilense* (Igic *et al.*, 2007) (Fig. 4). In the predicted mature protein sequences, there are only three nonconservative amino acid differences between hab-6 and the known functional S-RNases. The first, N to I, is located near C1 and is adjacent to a cysteine residue involved in disulfide bridge formation (Ida *et al.*, 2001). The second, S to N, is near the C2 region and the third, I to T, is located near the C4 region. None of these amino acid substitutions impact the predicted secondary structure of the protein when modeled to the crystal structure of the *Nicotiana alata* S-RNase SF11 (Ida *et al.*, 2001). However, it is still possible that they could impact activity through influencing local amino acid environments.

One striking difference between the deduced amino acids sequences is a putative 26 amino acid N-terminal extension which is present in hab-6 but lacking in S11 and S2. An *in silico* analysis suggests that this extension would disrupt the signal peptide required for secretion, and based on molecular weight (MW) calculations, a partially processed protein could explain the characteristic doublet seen in hab-6 immunoblots (Fig. 3). The putative extension is the result of a single base deletion placing an upstream ATG in-frame with the hab-6 open reading frame (ORF) (Fig. S2). However, we found that this upstream ATG (unlike the second ATG) does not conform with the Kozak consensus sequence, as it lacks a purine at the universally conserved -3 position (Hernández *et al.*, 2019). Further, peptide mass fingerprinting and immunoblot analyses using an antibody directed to the potential 26 aa N-terminal peptide failed to detect this alternative N-terminal peptide (data not shown).

Because sequence differences did not reveal an apparent explanation for the low activity associated with hab-6, we also

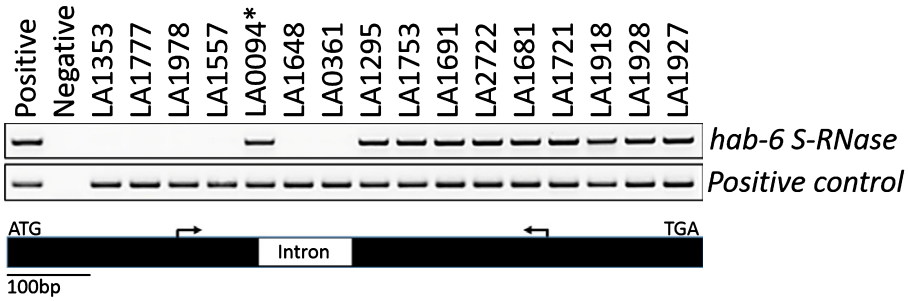

Fig. 2 Presence of the *hab-6S-RNase* allele in southern *Solanumhabrochaites* populations. Polymerase chain reaction (PCR) analysis of genomic DNA for the *hab-6* allele. Arrows in the schematic show primer locations. The asterisk (*) indicates that in population LA0094 the *hab-6* allele was only amplified in some individuals.

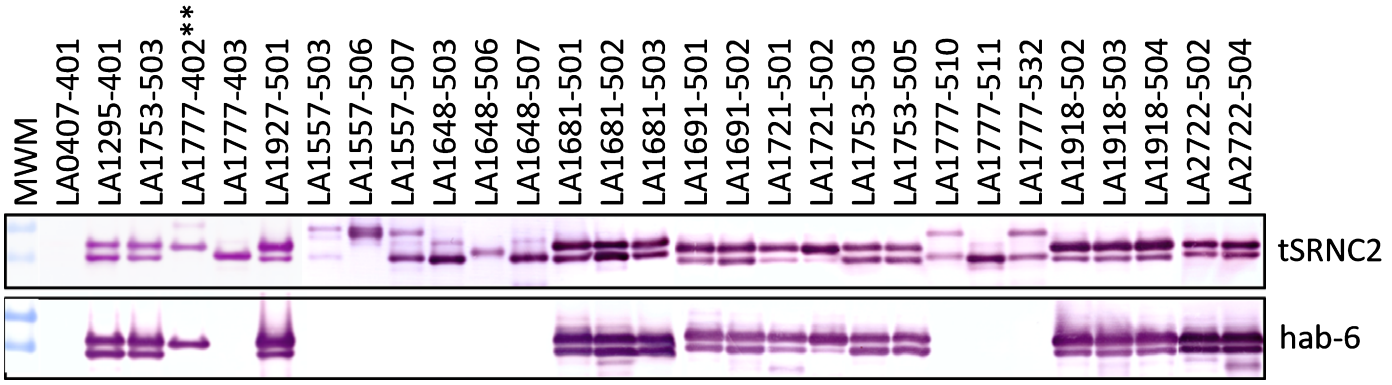

Fig. 3 Immunoblot of *Solanumhabrochaites* stylar extracts. Representative samples showing immunoblotting of stylar extracts from southern populations. Northern population LA0407 was used as a negative control, as it does not express S-RNase. hab-6, anti-peptide antibody designed to hab-6 S-RNase; MWM, molecular weight marker (lower band 26 kDa, upper band 35 kDa); tSRNC2, antibody to conserved domain 2 of S-RNase. The asterisks (**) indicate that the LA1777-402 cross reacts with the hab-6 antibody.

examined glycosylation which can impact S-RNase stability (Williams *et al.*, 2015) and could result in the doublet banding pattern. The hab-6 sequence contains two putative N-glycosylation sites (Fig. 4, denoted by the '^' symbol) that are conserved in *S. chilense* S2 and *S. peruvianum* S11 proteins. We performed a deglycosylation experiment with partially purified hab-6 S-RNase (Fig. 5a) and found that treatment with peptide-N-glycanase F collapses the doublet to a single band, suggesting the doublet is due to protein glycosylation and not to utilization of the upstream start codon. Further, we probed stylar extracts of an *S. chilense* plant known to contain the functional S2 S-RNase, side by side with stylar extracts from LA1927 and found that the S2 S-RNase also shows the characteristic doublet, suggesting a similar glycosylation status (Fig. 5b). Although not definitive, these results suggest that differential glycosylation is not the cause of low activity in hab-6. Together, these results do not provide a satisfactory explanation for the low activity of hab-6, which will require further study.

Stylar self-incompatibility factor HT-protein is lost to mutation in at least one population of southern self-compatible *Solanum habrochaites*

HT-protein is not encoded at the *S*-locus but is required for self-pollen tube rejection (Tovar-Mendez *et al.*, 2014). Therefore, we surveyed selected southern populations for this protein using immunoblotting. All populations showed a reactive band of the expected size for HT-protein, except for LA1691 (Fig. S3). These results suggest that the loss of HT-protein is not the reason for the SI to SC transition in southern *S. habrochaites* populations. Cloning and sequencing of the HT-gene showed a single base pair deletion leading to the formation of an early stop codon in LA1691 (Fig. S4). Since HT protein has roles in both SI and in interspecific reproductive barriers (Tovar-Mendez *et al.*, 2014, 2017) we tested whether styles of southern SC populations could reject pollen tubes of *S. lycopersicum*. We found that interspecific pollen tube rejection was robust in southern SC populations, including LA1691 (data not shown), indicating that hab-6 or another stylar factor is sufficient for interspecific pollen tube rejection in LA1691.

Mixed-mating population LA0094 segregates for the *hab-6* allele

Solanum habrochaites population LA0094 was of special interest because it is the northernmost population containing SC individuals. We found that the *hab-6* allele segregates in LA0094 (Table 2), making this population ideal for examining the relationship between *hab-6* and SC. To better understand the distribution of *S*-haplotypes in LA0094, we recovered sequences of three presumably functional *S-RNase* alleles in addition to *hab-6*. The first allele (*hab-9*) encodes an S-RNase that is over 97% identical to two previously identified *S. habrochaites* S-RNases: hab-4 from SI LA1353 and LhgSRN-1 from SC LA0407 (Covey *et al.*, 2010) (Fig. S5a). The second allele (*hab-10*) encodes an S-RNase that is 94% identical to the S-16 S-RNase from SI *S. chilense* (Fig. S5b). The third allele (*hab-11*) encodes an S-RNase that is 97% identical to the S3 S-RNase from SI *S. peruvianum* (Royo *et al.*, 1994) and the S15 S-RNase from SI *S. chilense* S15 (Igic *et al.*, 2007) (Fig. S5c).

We genotyped 21 LA0094 individuals using allele-specific primers for *hab-6*, *hab-9*, *hab-10* and *hab-11* and evaluated mating system of 11 of those individuals (Table S2). We found that all of the SC plants ($n = 7$) and none of the SI plants ($n = 4$) contained *hab-6* (Fig. 6 shows results from six individuals). Genotyping of 21 individuals showed that 62% (13/21) contained at least one copy of *hab-6*, and *hab-6* was detected both alone and in combination with all three of the functional *S-RNase* alleles (Table S2).

Our results with this small sample suggest that *hab-6* resides at the *S*-locus. To confirm this, we expanded our study by genotyping progeny of crosses using *hab-6*/*hab-10* heterozygous plants as pollen donors onto females with known *S-RNase* alleles. If *hab-6* is located at the *S*-locus, we would expect that half of the progeny from these crosses would harbor *hab-6* while the other half would contain the *hab-10* allele, and that none of the progeny would

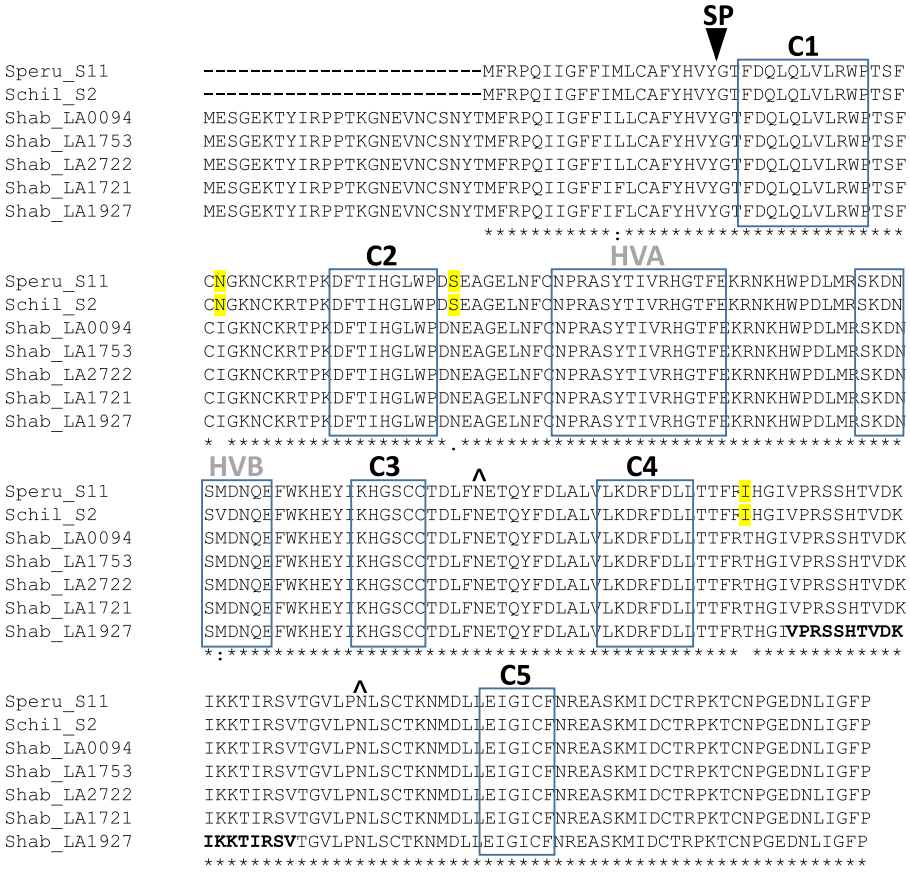

Fig. 4 Alignment of hab-6 S-RNase and related functional S-RNase amino acid sequences. Sequence conservation between hab-6 S-RNases from *Solanumhabrochaites* (Shab) and functional S-RNases from *Solanumperuvianum* (Speru S11) and *Solanumchilense* (Schil S2) are indicated by stars. The five conserved (C1–C5) and two hypervariable (HVA, HVB) regions of S-RNases are boxed. The amino acid sequence used to generate a specific anti-hab-6 antibody is highlighted in bold. GenBank numbers are as follows: Speru_S11, U28795; Schil_S2 (full length) MW183815; Shab_LA1927 (full length) MW183811; Shab_LA2722, MW183810; Shab_LA1753, MW183813; Shab_LA1721, MW183814; Shab_LA0094 MW183812. ^, potential N-linked glycosylation site; SP, putative signal peptide cleavage site.

contain both alleles. We analyzed 128 progeny plants and found that 77 contained the *hab-10* allele, 51 contained the *hab-6* allele, and none contained both alleles. The observed result (0, 77, 51) does not differ from the expected result (0, 64, 64) (Freeman–Halton extension of Fisher's exact test $P = 0.13$), consistent with a location of *hab-6* at the *S*-locus.

Pairing of the *hab-6* haplotype with different *S*-haplotypes can change mating systems and create an intrapopulation barrier

The *hab-6 S*-haplotype *is expected to contain a fully functional male component with a complete suite of SLF genes. In this case, we would predict that pollen of the hab-6* haplotype is compatible on pistils of all other *S*-haplotypes in the population. Consistent with this prediction, two phenotyped individuals in the LA0094 population with a *hab-6*/*hab-9* genotype were SC (Fig. 6; Table S2). In addition, we would predict that plants heterozygous for *hab-6* would show SI/SC codominance in self-crosses wherein both S-RNases are expressed but only pollen of the *hab-6* haplotype will successfully fertilize ovules, while pollen of the other haplotype is rejected.

To test these predictions, we crossed an SC individual homozygous for *hab-6* (LA0094-503) with a heterozygous *hab-9*/*hab-10* SI individual (LA0094-502). As predicted, when the SC *hab-6* homozygote was used as female, crosses were successful, and genotyping of the progeny showed that all progeny contained *hab-6*, half contained *hab-9* and half contained *hab-10* (Fig. 7a). However, when the SI individual was used as a female, crosses were not successful, and an analysis of pollen tube growth showed rejection of SC (*hab-6* homozygote) pollen tubes in SI pistils (Fig. 7b). These results demonstrate the presence of a unilateral crossing barrier that is due to pollen tube rejection.

To investigate this barrier further, we grew six F_1 plants from the successful cross (three of each genotype) to maturity to determine mating system type. All three *hab-6*/*hab-9* F_1 individuals were SC (Fig. 7c). A close analysis of pollen tube growth through self-pollinated styles showed that approximately half of the pollen tubes were rejected, suggesting that hab-9 is functioning in SI pollen rejection (Fig. 7c inset). Genotype analysis of F_2 progeny ($n = 60$) produced from self-pollinations of the SC F_1 (*hab-6*/*hab-9*) plants showed that 50% of individuals were heterozygous for *hab-6*/*hab-9* and 50% of individuals were homozygous for *hab-6*, and no plants were homozygous *hab-9*, which would be expected if hab-9 S-RNase is functional in SI and is only transmitted through female gametes (Fig. 7d shows genotypes of a subset of F_2 plants). Thus, the results for the F_1 *hab6*/*hab-9* plants mirror our predicted scenario of codominance and clearly indicate that *hab-6* pollen is fully competent in this cross. We also found that pollen from *hab-6* homozygotes was accepted by pistils of SI *S. habrochaites* LA1777 (data not shown) suggesting *hab-6* pollen is functional against multiple *S*-haplotypes.

By contrast, when we analyzed the *hab-6*/*hab-10* F_1 plants we found that all individuals were SI and exhibited rejection of self-

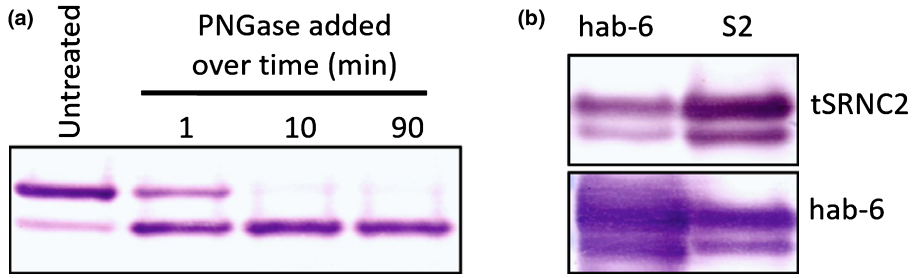

Fig. 5 Glycosylation in hab-6 S-RNase. (a) Deglycosylation of partially purified hab-6 S-RNase from *Solanum habrochaites* population LA1927. Over time, deglycosylase peptide-N-Glycanase (PNGase) collapses the characteristic protein doublet into a single band, consistent with variable glycosylation. (b) Immunoblotting shows that *Solanumchilense* plants containing the S2 S-RNase cross-react with the peptide antibody made to the *Solanumhabrochaites* hab-6 S-RNase and show a similar double banding pattern. tSRNC2 is an antibody made to the C2 conserved domain present in all S-RNase sequences.

pollen tubes (Fig. 7e). Pollen tube growth assays showed that the SC parent (*hab-6/hab-6*) accepted pollen tubes from all F_1 progeny, whereas the SI parent (*hab-9/hab-10*) rejected all pollen tubes from all F_1 progeny (data not shown). These results are consistent with the unidirectional intrapopulation barrier discovered in the parental cross and show that pistils expressing the *hab-10* haplotype reject pollen of the *hab-6* haplotype as well as pollen expressing the self (*hab-10*) haplotype.

Discussion

A single self-incompatibility to self-compatibility mating system transition at the southern species margin is associated with the *hab-6* haplotype

The molecular basis for the breakdown of SI is often elusive, even in well-studied systems like *Solanum*. Our previous work identified two distinct SI → SC transitions associated with different *S-RNase* mutations at the northern *S. habrochaites* species margin (Broz *et al.*, 2017b). By contrast, the present study shows that all southern SC *S. habrochaites* populations tested contained the *hab-6* haplotype, suggesting that a single SI → SC transition occurred at the southern species margin (Fig. 1).

The hab-6 protein was previously found to exhibit very low S-RNase activity using two different assays, and this low activity was hypothesized to result in the loss of SI (Covey *et al.*, 2010). In this study, we confirmed that *hab-6* segregates as expected for an allele of the *S*-locus and found that the sequence conforms to that of a functional S-RNase. We identified only three amino acid differences between mature hab-6 and closely related functional S-RNases (Fig. 4). One nonconservative change places a hydrophobic residue adjacent to a cysteine reside, and it is possible that it could interfere with disulfide bond formation, which is important in S-RNase secondary structure. However, further studies are required to test this hypothesis. Currently, the basis for the low activity of hab-6 remains enigmatic.

Previous work suggests that S-RNases can vary widely in specific activity and still function in SI (Zurek *et al.*, 1997). Thus, it is possible that factors other than hab-6 are responsible for the SC phenotype, although we eliminated loss of stylar SI factor HT as

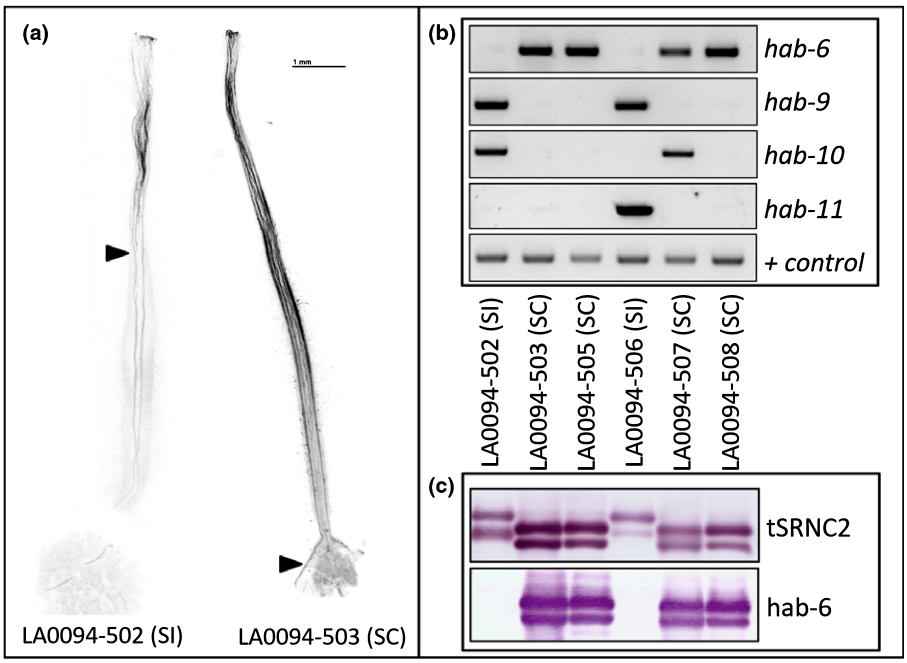

Fig. 6 Presence of the *hab-6* allele and hab-6 protein correlates with the self-compatibility (SC) phenotype in individuals of *Solanum habrochaites* population LA0094. (a) Self-pollen tube growth through styles, black arrowheads indicate the longest pollen tube; (b) amplification of the *hab-6*, *hab-9*, *hab-10* and *hab-11* alleles; (c) Western blot for S-RNase proteins using general (tSRNC2, top panel) and hab-6 specific (hab-6, bottom panel) S-RNase antibodies.

a cause. The correlation we observed between hab-6 and SC could point to other causative factors located at the *S*-locus (i.e. linked to *hab-6*). For example, a gain-of-function mutation in an *SLF* gene can result in recognition and detoxification of a self S-RNase, and this has been previously cited as the molecular basis for SC in *Petunia* (Sijacic *et al.*, 2004; Kubo *et al.*, 2015) and in *Solanum neorickii* (Markova *et al.*, 2017). It is not clear whether this type of mutation exists in the *hab-6* haplotype, since the complete suite of SLFs has not been fully documented in *S. habrochaites*, and specific interactions between SLF and S-RNase proteins are only beginning to be characterized.

Origin and spread of self-compatibility at the southern *Solanum habrochaites* species range margin

Theoretical and empirical studies suggest that when SC arises, it will rapidly spread due to the evolutionary forces of transmission advantage and reproductive assurance, unless inbreeding depression or pollen discounting are substantial (Fisher, 1941; Charlesworth & Charlesworth, 1979; Kalisz *et al.*, 2004; Porcher & Lande, 2005; Busch & Delph, 2012; Layman *et al.*, 2017). We have shown that a single SI to SC mating system transition took place in the southern species range of *S. habrochaites* and that SC has spread to fixation in populations that occupy nearly one quarter of the species range. The simplest interpretation of our population survey is that the SC-associated *hab-6* haplotype, with the *hab-6 S-RNase* allele and its linked *SLF* genes, arose in the Rio Chillon valley in Peru and spread southward to additional river valleys. However, other scenarios cannot be ruled out, as changing environmental and ecological factors are expected to influence the evolution and distribution of SC over time. For example, the SC haplotype may have arisen further south in Peru and established or invaded populations to the north, resulting in the current distribution.

Population genetic studies place all southern SC populations and the geographically close SI populations into a single genetic group, and estimated levels of heterozygosity are consistently low in the SC populations (Rick *et al.*, 1979; Sifres *et al.*, 2011; Landis *et al.*, 2021). Population bottlenecks are expected to occur as a species migrates, and this, combined with the appearance of SC, may have led to the observed declines in heterozygosity of southern SC populations. A reduction in population size during migrations of SI species is expected to result in mate limitation because only a small number of *S*-alleles will be present in founder individuals. In this scenario, natural selection should favor mutations that confer SC because SI individuals will have fewer outcross partners available due to the low diversity of *S*-alleles. Similarly, ecological factors create variable pollination environments that could favor increased rates of selfing. Future studies measuring selfing rates, inbreeding depression, and pollen discounting will be essential to understanding the extent to which different processes drive SC in *S. habrochaites*.

Population contraction during migration and reproductive assurance associated with selection for SC may have influenced

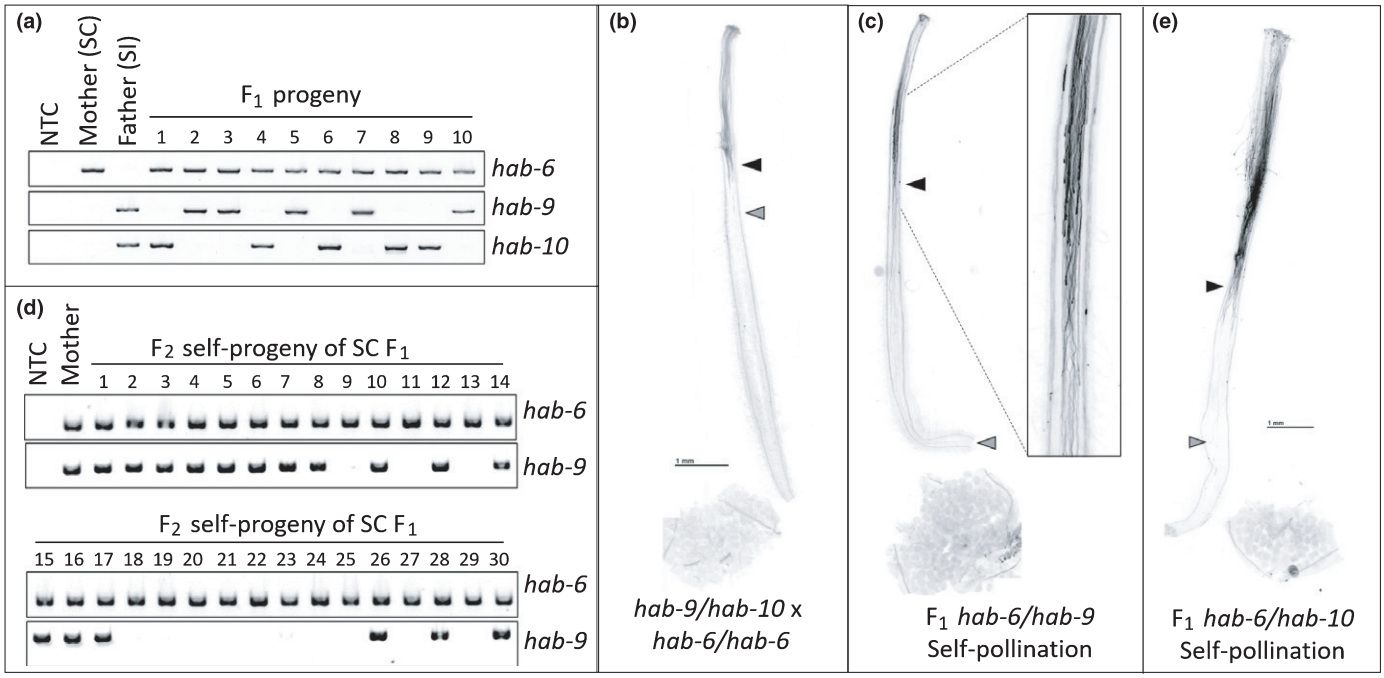

Fig. 7 Genotype and mating system analysis from an intrapopulation cross of *Solanumhabrochaites* population LA0094. (a) Genotype results for ten F_1 progeny from the successful LA0094 intrapopulation cross. (b) Pollen tube growth of an intrapopulation cross between LA0094-502 (*hab-9/hab-10*) as female and LA0094-503 (*hab6/hab-6*) as male. Black arrowheads indicate the area where many pollen tubes are rejected, and gray arrowheads indicate the location of the longest pollen tubes. (c) Pollen tube growth through styles of self-pollinated F_1 self-compatible (SC; *hab-6/hab-9*) progeny. The inset is an enlargement of a region where many (presumably *hab-9*) pollen tubes are rejected in SC F_1 plants. (d) Genotype results for 30 F_2 selfed progeny of SC F_1 (*hab-6/hab-9*). The absence of *hab-9* homozygotes suggests that *hab-9* is only transmitted through female gametes. (e) Pollen tube growth through styles of self-pollinated F_1 self-incompatible (SI; *hab-6/hab-10*) progeny. NTC, no template control.

the spread of the *hab-6* allele. However, our data from population LA0094 highlight an additional feature of S-RNase-based gametophytic SI that is often not explicitly considered: the speed at which an SC mutation can become fixed in a population. Under the non-self-recognition model, mutations conferring SC are expected to be phenotypically co-dominant within a single generation, as we observed in *hab-6/hab-9* heterozygotes (Fig. 7). This creates a 2 : 1 advantage for the *hab-6* haplotype over the *hab-9* haplotype, which can only be transmitted through the female. For example, if a single heterozygous plant of this type (i.e. *hab-6/hab-9*) was the founder of a population, the *hab-6* allele would rapidly spread to fixation even if outcrossing occurred in subsequent generations. Assuming no pollen or seed discounting, the frequency of the *hab-9* allele would be reduced to < 1% after only four generations of selfing (*hab-9* initial frequency = 0.25, after four generations (0.25^4) its frequency is reduced to 0.004).

This contrasts with the self-recognition system of sporophytic SI in which the pollen and pistil both express two different haplotypes, and the interaction of any pair of self-pollen and pistil factors blocks pollen tube germination. In this case, a loss of function mutation in either a male or female factor will generally be recessive, although some dominant mutations have been shown to confer SC (Bachmann *et al.*, 2019). In the case of a recessive mutation, an SC individual will be generated after a minimum of two generations of outcrossing. In S-RNase-based gametophytic SI, the rapid establishment of SC alleles may constitute an additional evolutionary advantage for SC mutations.

Persistence of self-incompatibility alleles in the face of self-compatibility mutations

Plant populations containing mixed SI/SC mating systems are common, but the mechanisms through which these populations persist remains a puzzle in evolutionary biology. In some cases, the maintenance of mixed mating systems can be explained by pollination ecology and relative rates of outcrossing, which can vary over time (Kalisz *et al.*, 2004; Goodwillie *et al.*, 2005). In the cases of *S. habrochaites* population LA0094, it is possible that gene flow from neighboring populations influences the balance of *hab-6* relative to other *S*-alleles. Here, population dynamics of both *S. habrochaites* and its pollinators are expected to influence interpopulation gene flow and the stability of mixed mating.

Although temporal and ecological factors likely play important roles in the persistence of mixed mating populations, our results suggest a genetic mechanism that could also allow for the maintenance of both SC and SI haplotypes. We found that pollen of *hab-6* homozygotes is rejected by pistils of *hab-9/hab-10* heterozygotes, but the reciprocal cross is compatible, revealing a unidirectional intrapopulation barrier in population LA0094. We further found that this barrier is associated with the *hab-10* haplotype, since *hab-6/hab-10* heterozygotes are SI. The simplest explanation for these results is that pollen with the *hab-6* haplotype does not express a complete set of SLF proteins, rendering it unable to recognize and detoxify hab-10. In this case, any female expressing the *hab-10* haplotype will reject pollen of the *hab-6* haplotype, and pistils of *hab-6/hab-10* heterozygotes will reject pollen tubes of either *S*-haplotype resulting in SI. Given these findings, it is intriguing to consider the possibility that the SC *hab-6* haplotype invaded the LA0094 population after originating further south but could not spread to fixation due to the presence of the *hab-10* (and perhaps additional) resistant haplotypes.

Although the observed intrapopulation barrier can be most readily explained by the *hab-6* haplotype lacking a full suite of functional SLF genes, there are at least two other possible explanations. One is that *hab-10* encodes a 'dual specificity' S-RNase. Previous studies have shown that engineered changes in an S-RNase protein can lead to an unusual *S*-haplotype that rejects pollen tubes from both self and one additional haplotype (Matton *et al.*, 1999; Soulard *et al.*, 2013). However, to our knowledge, this type of dual-specificity S-RNase has never been identified in a natural population. A second explanation is that the *S*-locus of the *hab-6 S-RNase* contains the *SLF* suite from the *hab-10* haplotype. Pollen of this 'chimeric' *S*-haplotype would be able unable to recognize and detoxify hab-10, resulting in SI *hab-6/hab-10* heterozygotes. Interestingly, in this scenario, a plant homozygous for the chimeric *S*-haplotype would be SC, even if the low-activity hab-6 protein is a fully functional S-RNase, because the hab-10 SLF suite would recognize and detoxify hab-6. Thus, pollen of the chimeric *S*-haplotype would be compatible on any female in the population except those containing hab-10. The existence of a chimeric *S*-locus is theoretically unlikely, as the *S*-locus is located in heterochromatin and is not expected to undergo recombination. However, S-locus duplications have been reported that lead to unexpected inter-population and interspecific barriers in the Brassicaceae (Chantha *et al.*, 2013; Takada *et al.*, 2017). More studies are warranted to fully understand the molecular basis of incompatibilities in this population.

Conclusions

In summary, we identified a single SI → SC mating system transition at the southern species margin of *S. habrochaites* that is strongly correlated with the presence of an *S*-haplotype encoding hab-6, a low-activity S-RNase. We have empirically shown that the *hab-6* haplotype acts in the expected co-dominant fashion when paired with a functional *S*-haplotype, which could lead to rapid spread and fixation of SC. Further, we propose a genetic model by which an SC haplotype can be maintained within a population without spreading to fixation. If an SC haplotype is associated with an incomplete suite of SLFs that render it unable to recognize and detoxify all S-RNases within the population, this will create an intrapopulation barrier and provide a disadvantage for the SC haplotype as male. Thus, a balance between the array of functional SLFs of the SC *S*-haplotype and the array of resistant or susceptible S-RNases in a population may determine whether an SC mutation spreads to fixation when it arises within, or invades, an existing SI population.

Acknowledgements

The authors would like to thank Amy Boczon and Laura Hantzis for their help with field work, and Olivia Todd, Aleshia Martin,

Rachel Sharn and Nicole Irace for help imaging pollen tube growth through styles. This work was supported by US National Science Foundation grant MCB1127059.

Author contributions

AKB, AS-VD and PAB designed the research. AKB, AS-VD, AT-M, BM and PAM performed the research. AKB, AS-VD, AT-M and MWH collected the data. AKB, AT-M and MWH analyzed the data. AKB, AT-M, BM and PAB interpreted the data. AKB and PAB wrote the manuscript. All authors edited and approved the manuscript.

ORCID

Patricia A. Bedinger https://orcid.org/0000-0002-2769-5063
Amanda K. Broz https://orcid.org/0000-0001-5663-3569
Matthew W. Hahn https://orcid.org/0000-0002-5731-8808

Data availability

The data that support the findings of this study are openly available in the GenBank database at https://www.ncbi.nlm.nih.gov/genbank/, reference numbers MW183815; MW183811; MW183810; MW183813; MW183814; MW183812; MW183818; NCBI SRA database PRJNA310635.

References

Allen AM, Hiscock SJ. 2008. Evolution and phylogeny of self-incompatibility systems in angiosperms. In: Franklin-Tong VE, ed. *Self-incompatibility in flowering plants – evolution, diversity, and mechanisms*. Berlin/Heidelberg, Germany: Springer-Verlag, 73–101.

Almagro Armenteros JJ, Salvatore M, Emanuelsson O, Winther O, von Heijne G, Elofsson A, Nielsen H. 2019. Detecting sequence signals in targeting peptides using deep learning. *Life Science Alliance* **2**: e201900429.

Bachmann JA, Tedder A, Laenen B, Fracassetti M, Désamoré A, Lafon-Placette C, Steige KA, Callot C, Marande W, Neuffer B *et al.* 2019. Genetic basis and timing of a major mating system shift in *Capsella*. *New Phytologist* **224**: 505–517.

Baker HG. 1955. Self compatibility and establishment after long distance dispersal. *Evolution* **9**: 347–349.

Baker HG. 1967. Support for Baker's law–as a rule. *Evolution* **21**: 853.

Barrett SCH, Arunkumar R, Wright SI. 2014. The demography and population genomics of evolutionary transitions to self-fertilization in plants. *Philosophical Transactions of the Royal Society of London. Series B: Biological Sciences* **369**: 9.

Bedinger PA, Broz AK, Tovar-Mendez A, McClure B. 2017. Pollen–pistil interactions and their role in mate selection. *Plant Physiology* **173**: 79–90.

Broz AK, Guerrero RF, Randle AM, Baek YS, Hahn MW, Bedinger PA. 2017a. Transcriptomic analysis links gene expression to unilateral pollen–pistil reproductive barriers. *BMC Plant Biology* **17**: 81.

Broz AK, Randle AM, Sianta SA, Tovar-Mendez A, McClure B, Bedinger PA. 2017b. Mating system transitions in *Solanum habrochaites* impact interactions between populations and species. *New Phytologist* **213**: 440–454.

Busch JW, Delph LF. 2012. The relative importance of reproductive assurance and automatic selection as hypotheses for the evolution of self-fertilization. *Annals of Botany* **109**: 553–562.

Busch JW, Schoen DJ. 2008. The evolution of self-incompatibility when mates are limiting. *Trends in Plant Science* **13**: 128–136.

Chalivendra SC, Lopez-Casado G, Kumar A, Kassenbrock AR, Royer S, Tovar-Mendez A, Covey PA, Dempsey LA, Randle AM, Stack SM *et al.* 2013. Developmental onset of reproductive barriers and associated proteome changes in stigma/styles of *Solanum pennellii*. *Journal of Experimental Botany* **64**: 265–279.

Chantha SC, Herman AC, Platts AE, Vekemans X, Schoen DJ. 2013. Secondary evolution of a self-incompatibility locus in the Brassicaceae genus *Leavenworthia*. *PLoS Biology* **11**: e1001560.

Charlesworth D. 2003. Effects of inbreeding on the genetic diversity of populations. *Philosophical Transactions of the Royal Society of London Series B: Biological Sciences* **358**: 1051–1070.

Charlesworth D, Charlesworth B. 1979. The evolution and breakdown of S-allele systems. *Heredity* **43**: 41–55.

Charlesworth D, Wright SI. 2001. Breeding systems and genome evolution. *Current Opinion in Genetics & Development* **11**: 685–690.

Covey PA, Kondo K, Welch L, Frank E, Sianta S, Kumar A, Nuñez R, Lopez-Casado G, Van Der Knaap E, Rose JKC *et al.* 2010. Multiple features that distinguish unilateral incongruity and self-incompatibility in the tomato clade. *The Plant Journal* **64**: 367–378.

Darwin CR. 1876. *The effects of cross and self-fertilisation in the vegetable kingdom*. London, UK: J. Murray.

Fisher RA. 1941. Average excess and average effect of a gene substitution. *Annals of Eugenics* **11**: 53–63.

Fujii S, Kubo K, Takayama S. 2016. Non-self- and self-recognition models in plant self-incompatibility. *Nature Plants* **2**: 9.

Goldberg EE, Igić B. 2012. Tempo and mode in plant breeding system evolution. *Evolution* **66**: 3701–3709.

Goldberg EE, Kohn JR, Lande R, Robertson KA, Smith SA, Igić B. 2010. Species selection maintains self-incompatibility. *Science* **330**: 493–495.

Goldraij A, Kondo K, Lee CB, Hancock CN, Sivaguru M, Vazquez-Santana S, Kim S, Phillips TE, Cruz-Garcia F, McClure B. 2006. Compartmentalization of S-RNase and HT-B degradation in self-incompatible *Nicotiana*. *Nature* **439**: 805–810.

Goodwillie C, Kalisz S, Eckert CG. 2005. The evolutionary enigma of mixed mating systems in plants: occurrence, theoretical explanations, and empirical evidence. *Annual Review of Ecology, Evolution, and Systematics* **36**: 47–79.

Hancock CN, Kent L, McClure BA. 2005. The stylar 120 kDa glycoprotein is required for *S*-specific pollen rejection in *Nicotiana*. *The Plant Journal* **43**: 716–723.

Hernández G, Osnaya VG, Pérez-Martínez X. 2019. Conservation and variability of the AUG initiation codon context in eukaryotes. *Trends in Biochemical Sciences* **44**: 1009–1021.

Ida K, Shinkawa T, Norioka S, Newbigin E, Clarke AE, Sakiyama F, Sato M. 2001. Crystallization and preliminary X-ray crystallographic analysis of S-allelic glycoprotein SF11-RNase from *Nicotiana alata*. *Acta Crystallographica Section D: Biological Crystallography* **57**: 143–144.

Igic B, Bohs L, Kohn JR. 2006. Ancient polymorphism reveals unidirectional breeding system shifts. *Proceedings of the National Academy of Sciences, USA* **103**: 1359–1363.

Igic B, Busch JW. 2013. Is self-fertilization an evolutionary dead end? *New Phytologist* **198**: 386–397.

Igic B, Lande R, Kohn JR. 2008. Loss of self-incompatibility and its evolutionary consequences. *International Journal of Plant Sciences* **169**: 93–104.

Igic B, Smith WA, Robertson KA, Schaal BA, Kohn JR. 2007. Studies of self-incompatibility in wild tomatoes: I. S-allele diversity in *Solanum chilense* Dun. (Solanaceae). *Heredity* **99**: 553–561.

Jiménez-Durán K, McClure B, García-Campusano F, Rodríguez-Sotres R, Cisneros J, Busot G, Cruz-García F. 2013. NaStEP: A proteinase inhibitor essential to self-incompatibility and a positive regulator of HT-B stability in *Nicotiana alata* pollen tubes. *Plant Physiology* **161**: 97–107.

Kalisz S, Vogler DW, Hanley KM. 2004. Context-dependent autonomous self-fertilization yields reproductive assurance and mixed mating. *Nature* **430**: 884–887.

Kubo K-i, Entani T, Takara A, Wang N, Fields Am, Hua Z, Toyoda M, Kawashima S-i, Ando T, Isogai A *et al.* 2010. Collaborative non-self recognition system in S-RNase-based self-incompatibility. *Science* **330**: 796–799.

Kubo K-i, Paape T, Hatakeyama M, Entani T, Takara A, Kajihara K, Tsukahara M, Shimizu-Inatsugi R, Shimizu KK, Takayama S. 2015. Gene duplication and genetic exchange drive the evolution of S-RNase-based self-incompatibility in *Petunia*. *Nature Plants* **1**: 14005.

Lande R, Schemske DW. 1985. The evolution of self-fertilization and inbreeding depression in plants. 1. Genetic models. *Evolution* **39**: 24–40.

Landis JB, Miller CM, Broz AK, Bennett AA, Carrasquilla-Garcia N, Cook DR, Last RL, Bedinger PA, Moghe GD. 2021. Migration through a major Andean ecogeographic disruption as a driver of genetic and phenotypic diversity in a wild tomato species. *Molecular Biology and Evolution*: msab092.

Layman NC, Fernando MTR, Herlihy CR, Busch JW. 2017. Costs of selfing prevent the spread of a self-compatibility mutation that causes reproductive assurance. *Evolution* **71**: 884–897.

Li W, Chetelat RT. 2014. The role of a pollen-expressed Cullin1 protein in gametophytic self-incompatibility in *Solanum*. *Genetics* **196**: 439–442.

Li W, Chetelat RT. 2015. Unilateral incompatibility gene *ui1.1* encodes an S-locus F-box protein expressed in pollen of Solanum species. *Proceedings of the National Academy of Sciences, USA* **112**: 4417–4422.

Madeira F, Park Ym, Lee J, Buso N, Gur T, Madhusoodanan N, Basutkar P, Tivey ARN, Potter SC, Finn RD *et al.* 2019. The EMBL-EBI search and sequence analysis tools APIs in 2019. *Nucleic Acids Research* **47**: W636–W641.

Markova DN, Petersen JJ, Qin XQ, Short DR, Valle MJ, Tovar-Mendez A, McClure BA, Chetelat RT. 2016. Mutations in two pollen self-incompatibility factors in geographically marginal populations of *Solanum habrochaites* impact mating system transitions and reproductive isolation. *American Journal of Botany* **103**: 1847–1861.

Martin FW. 1963. Distribution and interrelationships of incompatibility barriers in *Lycopersicon hirsutum* Humb and Bonpl complex. *Evolution* **17**: 519–528.

Markova DN, Petersen JJ, Yam SE, Corral A, Valle MJ, Li W & Chetelat RT. 2017. Evolutionary history of two pollen self-incompatibility factors reveals alternate routes to self-compatibility within Solanum. *American Journal of Botany* **104**: 1904–1919.

Matton DP, Luu DT, Xike Q, Laublin G, O'Brien M, Maes O, Morse D, Cappadocia M. 1999. Production of an S RNase with dual specificity suggests a novel hypothesis for the generation of new *S* alleles. *Plant Cell* **11**: 2087–2097.

McClure B, Cruz-Garcia F, Romero C. 2011. Compatibility and incompatibility in S-RNase-based systems. *Annals of Botany* **108**: 647–658.

McClure BA, Haring V, Ebert PR, Anderson MA, Simpson RJ, Sakiyama F, Clarke AE. 1989. Style self-incompatibility gene products of *Nicotlana alata* are ribonucleases. *Nature* **342**: 955–957.

McClure B, Mou B, Canevascini S, Bernatzky R. 1999. A small asparagine-rich protein required for *S*-allele-specific pollen rejection in *Nicotiana*. *Proceedings of the National Academy of Sciences, USA* **96**: 13548–13553.

Miller CM. 2018. *Mating system transitions impact population structure and biodiversity in* Solanum habrochaites. MSc thesis, Colorado State University, Fort Collins, CO, USA.

Miller JS, Kostyun JL. 2011. Functional gametophytic self-incompatibility in a peripheral population of *Solanum peruvianum* (Solanaceae). *Heredity* **107**: 30–39.

de Nettancourt D. 1977. *Incompatibility in angiosperms*. Berlin, Germay: Springer-Verlag.

Pannell JR, Auld JR, Brandvain Y, Burd M, Busch JW, Cheptou P-O, Conner JK, Goldberg EE, Grant A-G, Grossenbacher DL *et al.* 2015. The scope of Baker's law. *New Phytologist* **208**: 656–667.

Peralta IE, Spooner DM, Knapp S. 2008. Taxonomy of wild tomatoes and their relatives (*Solanum* sect. *Lycopersicoides*, sect. *Juglandifolia*, sect. *Lycopersicon*; Solanaceae). *Systematic Botany Monographs* **84**: 83–89.

Porcher E, Lande R. 2005. Loss of gametophytic self-incompatibility with evolution of inbreeding depression. *Evolution* **59**: 46–60.

Ramanauskas K, Igić B. 2017. The evolutionary history of plant T2/S-type ribonucleases. *PeerJ* **5**: e3790.

Rick CM, Chetelat RT. 1991. The breakdown of self-incompatibility in *Lycopersicon hirsutum*. In: Hawkes L, Nee E, eds. *Solanaceae III: taxonomy, chemistry, evolution*. London, UK: Royal Botanic Gardens Kew and Linnean Society of London, 253–256.

Rick CM, Foves JF, Tanksley SD. 1979. Evolution of mating systems in *Lycopersicon hirsutum* as deduced from genetic variation in electrophoretic and morphological characters. *Plant Systematics and Evolution* **132**: 279–298.

Royo J, Kowyama Y, Clarke AE. 1994. Cloning and nucleotide sequence of two S-RNases from *Lycopersicon peruvianum* (L.) mill. *Plant Physiology* **105**: 751–752.

Sifres A, Blanca J, Nuez F. 2011. Pattern of genetic variability of *Solanum habrochaites* in its natural area of distribution. *Genetic Resources and Crop Evolution* **58**: 347–360.

Sijacic P, Wang X, Skirpan AL, Wang Y, Dowd PE, McCubbin AG, Huang S, Kao T-h. 2004. Identification of the pollen determinant of S-RNase-mediated self-incompatibility. *Nature* **429**: 302–305.

Silva NF, Goring DR. 2001. Mechanisms of self-incompatibility in flowering plants. *Cellular and Molecular Life Sciences* **58**: 1988–2007.

Soulard J, Qin X, Boivin N, Morse D, Cappadocia M. 2013. A new dual-specific incompatibility allele revealed by absence of glycosylation in the conserved C2 site of a *Solanum chacoense* S-RNase. *Journal of Experimental Botany* **64**: 1995–2003.

Stebbins GL. 1974. *Flowering plants: evolution above the species level*. Cambridge, UK: Belknap Press.

Steinbachs JE, Holsinger KE. 2002. S-RNase mediated gametophytic self-incompatibility is ancestral in eudicots. *Molecular Biology and Evolution* **19**: 825–829.

Stone JL, VanWyk EJ, Hale JR. 2014. Transmission advantage favors selfing allele in experimental populations of self-incompatible *Witheringia solanacea* (solanaceae). *Evolution* **68**: 1845–1855.

Takada Y, Murase K, Shimosato-Asano H, Sato T, Nakanishi H, Suwabe K, Shimizu KK, Lim YP, Takayama S, Suzuki Go *et al.* 2017. Duplicated pollen-pistil recognition loci control intraspecific unilateral incompatibility in *Brassica rapa*. *Nature Plants* **3**: 17096.

Takayama S, Isogai A. 2005. Self-incompatibility in plants. *Annual Review of Plant Biology* **56**: 467–489.

Tovar-Mendez A, Kumar A, Kondo K, Ashford A, Baek YS, Welch L, Bedinger PA, McClure BA. 2014. Restoring pistil-side self-incompatibility factors recapitulates an interspecific reproductive barrier between tomato species. *The Plant Journal* **77**: 727–736.

Tovar-Mendez A, Lu L, McClure B. 2017. HT proteins contribute to S-RNase-independent pollen rejection in *Solanum*. *The Plant Journal* **89**: 718–729.

Vallejo-Marín M, Walker C, Friston-Reilly P, Solís-Montero L, Igic B. 2014. Recurrent modification of floral morphology in heterantherous *Solanum* reveals a parallel shift in reproductive strategy. *Philosophical Transactions of the Royal Society of London Series B: Biological Sciences* **369**: 20130256.

Waterhouse A, Bertoni M, Bienert S, Studer G, Tauriello G, Gumienny R, Heer FT, de Beer TAP, Rempfer C, Bordoli L *et al.* 2018. SWISS-MODEL: homology modelling of protein structures and complexes. *Nucleic Acids Research* **46**: W296–W303.

Williams JS, Der JP, dePamphilis CW, Kao TH. 2014. Transcriptome analysis reveals the same 17 *S*-locus F-box genes in two haplotypes of the self-incompatibility locus of *Petunia inflata*. *Plant Cell* **26**: 2873–2888.

Williams JS, Wu L, Li S, Sun P, Kao TH. 2015. Insight into S-RNase-based self-incompatibility in *Petunia*: recent findings and future directions. *Frontiers in Plant Science* **6**: 41.

Wright SI, Kalisz S, Slotte T. 2013. Evolutionary consequences of self-fertilization in plants. *Proceedings of the Royal Society B: Biological Sciences* **280**: 20130133.

Wu L, Williams JS, Sun L, Kao TH. 2020. Sequence analysis of the *Petunia inflata* S-locus region containing 17 S-Locus F-Box genes and the S-RNase gene involved in self-incompatibility. *The Plant Journal* **104**: 1348–1368.

Zhao L, Huang J, Zhao Z, Li Q, Sims TL, Xue Y. 2010. The Skp1-like protein SSK1 is required for cross-pollen compatibility in S-RNase-based self-incompatibility. *The Plant Journal* **62**: 52–63.

Zurek DM, Mou B, Beecher B, McClure B. 1997. Exchanging sequence domains between S-RNases from *Nicotiana alata* disrupts pollen recognition. *The Plant Journal* **11**: 797–808.

Supporting Information

Additional Supporting Information may be found online in the Supporting Information section at the end of the article.

Fig. S1 Alignment of deduced amino acid sequences of hab-6 and an S-RNase from LA1777.

Fig. S2 Alignment of related functional and *hab-6* S-RNase nucleotide sequences.

Fig. S3 HT-protein presence in stylar extracts of southern *Solanum habrochaites* populations.

Fig. S4 Alignment of the *HT-A* sequence from *Solanum habrochaites* populations.

Fig. S5 Alignments of S-RNase sequences detected in *Solanum habrochaites* population LA0094.

Methods S1 Transcriptome analysis of stylar RNA from *Solanum habrochaites* population LA2722.

Table S1 Primer sequences.

Table S2 Genotype and mating system data for 21 LA0094 individuals.

Please note: Wiley Blackwell are not responsible for the content or functionality of any Supporting Information supplied by the authors. Any queries (other than missing material) should be directed to the *New Phytologist* Central Office.